

**MONITORING POWER PLANT EFFICIENCY USING THE MICROWAVE-EXCITED
PHOTOACOUSTIC EFFECT TO MEASURE UNBURNED CARBON**

Quarterly Technical Progress Report

Reporting Period Start Date: October 1, 2002
Reporting Period End Date: December 31, 2002

Principal Author(s):
Robert C. Brown, Robert J. Weber, and Andrew A. Suby

Date Report Issued:
January 2003

DOE Award Number:
DE-FC22-01NT41220

Submitted By:
Center for Sustainable Environmental Technologies
Iowa State University
285 Metals Development Bldg.
Ames, IA 50011-3020

DISCLAIMER

This report was prepared as an account of work sponsored by an agency of the United States Government. Neither the United States Government nor any agency thereof, nor any of their employees, makes any warranty, express or implied, or assumes any legal liability or responsibility for the accuracy, completeness, or usefulness of any information, apparatus, product, or process disclosed, or represents that its use would not infringe privately owned rights. Reference herein to any specific commercial product, process, or service by trade name, trademark, manufacturer, or otherwise does not necessarily constitute or imply its endorsement, recommendation, or favoring by the United States Government or any agency thereof. The views and opinions of authors expressed herein do not necessarily state or reflect those of the United States Government or any agency thereof.

ABSTRACT

Three test instruments are being evaluated to determine the feasibility of using photo-acoustic technology for measuring unburned carbon in fly ash. The first test instrument is a single microwave frequency system previously constructed to measure photo-acoustic signals in an off-line configuration. This system was assembled and used to test parameters thought important to photo-acoustic signal output. A standard modulation frequency was chosen based upon signal to noise data gained from experimentation. Sample heterogeneity was tested and found not to be influential. Further testing showed that sample compression and photo-acoustic volume do affect photo-acoustic signal with photoacoustic volume being the most influential. Testing in the fifth quarter focused on microwave power stability.

Simultaneously, a second instrument is being constructed based in part on lessons learned with the first instrument, but also expands the capabilities of the first instrument by allowing a spectrum of microwave frequencies to be tested up to 10 GHz. The power amplifiers for this second instrument were completed and tested. Improvements were made to the current leveling loop, which will stabilize the microwave power. This loop is currently in operation with the single frequency cell. Discriminatory measurements are continuing in an attempt to differentiate between magnetic contaminants such as iron and non-magnetic contaminants such as carbon. A short coaxial test fixture was fabricated and tested showing the promise of another microwave based test method for determining carbon content in fly ash. Preliminary design iterations for the third on-line instrument (based on the experiences of the first two instruments) have begun.

Keywords: fly ash, carbon monitor, unburned carbon, boiler instrumentation

TABLE OF CONTENTS

DISCLAIMER	ii
ABSTRACT	iii
INTRODUCTION	1
EXPERIMENTAL	1
The Single Microwave Frequency, Off-Line Instrument	1
The Microwave Spectrometer	2
The On-line Monitor	3
RESULTS AND DISCUSSION	7
The Single Microwave Frequency, Off-Line Instrument	7
The Microwave Spectrometer	8
The On-line Monitor	14
CONCLUSION	15
REFERENCES	15

INTRODUCTION

The objective of this project is to explore the use of the microwave-excited photoacoustic (MEPA) effect for quantitative analysis of granular and powdered materials. The focal point of the research centers on the measurement of unburned carbon in fly ash, an important parameter in the electric utility industry used to determine plant efficiencies. The culmination of this project will be an on-line carbon-in-ash monitor for coal-fired power plants. However, evaluations will be made on other powdered solids, particularly coal.

The approach to this project includes work with three MEPA instruments. The first instrument is a single microwave frequency, off-line instrument built at Iowa State University as part of proof-of-concept evaluations. It is being used to evaluate precision and accuracy of the MEPA technique. The second instrument is being constructed as a microwave spectrometer based on MEPA. It will be used to evaluate a variety of industrial important powders, including fly ash and pulverized coal. The final instrument will be built based on the results of work with the previous two instruments and will be used as an on-line monitor of unburned carbon in fly ash.

EXPERIMENTAL

The Single Microwave Frequency, Off-Line Instrument

Testing was continued to determine parameters that affect photo-acoustic measurement accuracy and precision. Variables examined (to date) which may influence the photo-acoustic signal include: sample heterogeneity, sample bulk density, sample compression, sample moisture content, modulation frequency, signal to noise ratio, and photoacoustic volume. Ambient temperature and humidity were also examined. Current focus is on microwave power stability.

The Microwave Spectrometer

As indicated in the fourth quarterly report, the microwave spectrometer sources for 0.5 to 4 GHz and 4 GHz to 10 GHz were completed last quarter. This quarter the microwave work concentrated on using the sources to make measurements. Figure RJW-1 is shown again from the previous report and shows the current configuration of the power sources.

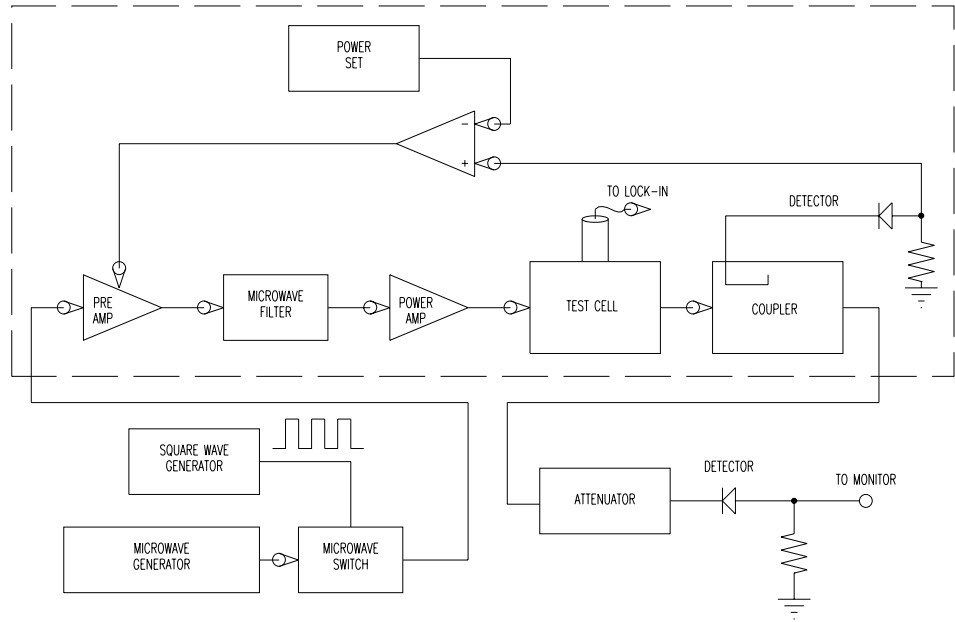


Figure RJW-1: Leveled Amplifier System

The measurements for the microwave system largely concentrated on making electric field versus magnetic field measurements. In addition to those measurements, some investigation of post-processing the lock-in amplifier data was done.

The On-line Monitor

The third phase of this work is to design an on-line carbon monitor based on the microwave-excited photoacoustic effect. The original concept is illustrated in Fig. 1. In this arrangement, fly ash flows between the striplining and one of the duct walls. Acoustical access through this wall allows a microphone to detect the photoacoustic signal.

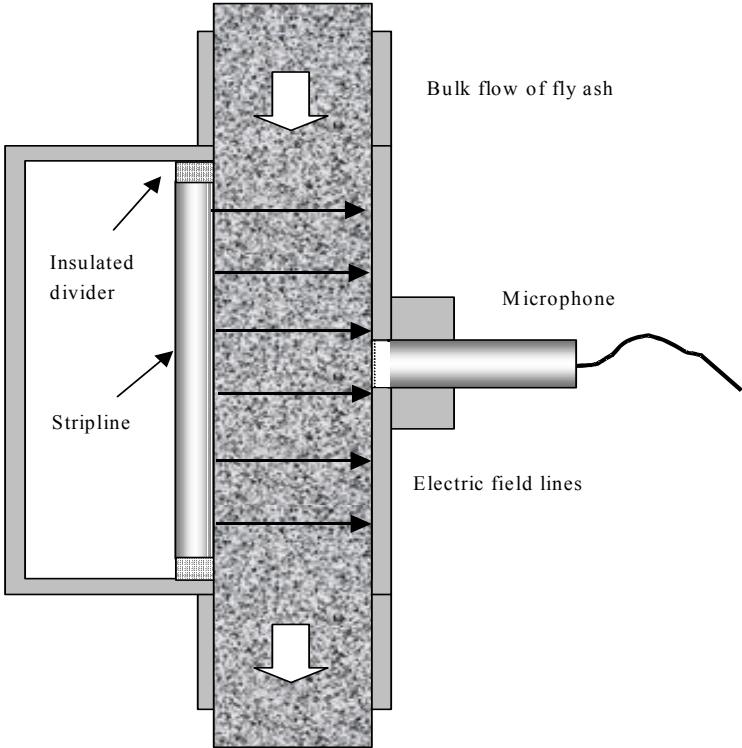


Fig. 1. Concept for on-line carbon in ash monitor

Testing in phase I revealed a difficulty with this original design: the photoacoustic signal is strongly dependent on the volume of gas between the granular sample and the microphone face. Since this volume would be difficult to control in the presence of flowing particles, precision of the photoacoustic signal would suffer.

We investigated changes in signal detection that would avoid this difficulty. We determined that instead of detecting the thermal acoustic wave generated in the gas volume, it would be better to detect the thermal elastic wave that is generated in the presence of microwave excitation. The thermal elastic wave arises from the periodic volume expansion of the bulk sample as a result of periodic heating (as opposed to the production of an acoustic wave at the

surface of the sample). The pressure, P, arising in the sample as a result of this thermal elastic wave is given by:

$$P = B\alpha_t\bar{\theta} \quad (1)$$

where B is the bulk modulus of the solid sample, α_t is the coefficient of thermal expansion, and $\bar{\theta}$ is the average temperature rise in the sample. We estimate for present B to be 5×10^7 dyne/cm² from information available from the study of grains in hoppers and α_t is about 9×10^{-6} °C⁻¹ from data on silica. The average temperature rise is calculated from an energy balance on the sample:

$$\bar{\theta} = \frac{\dot{W}_o[1 - \exp(-\beta\mu)] / \omega}{\rho C \mu A} \quad (2)$$

where \dot{W}_o is the incident microwave power (1 W), β is the absorptivity of fly ash to microwave radiation, μ is the distance over which the microwaves are absorbed, ω is the modulation frequency (20 Hz), ρ is the density of the bulk powder (2.6 g/cm³), C is the heat capacity of the solid particles (0.69 J/g °C), and A is the cross-sectional area of irradiation.

For low absorptivity, which is inherent in the microwave-excited photoacoustic effect, Eq. 2 reduces to:

$$\bar{\theta} \approx \frac{\dot{W}_o\beta}{\rho CA\omega} \quad (3)$$

The absorptivity for fly ash was estimated from measurements on the Phase I instrument. These tests found that 5 mW of the incident 1 W of microwave radiation was absorbed for every 1% carbon content of the fly ash over a sample depth of 2.5 cm. Accordingly,

$$\beta = -\ln(1 - \dot{W} / \dot{W}_o) / \mu = -\ln(1 - 5 \times 10^{-3} / 1) / 0.025 = 0.20 \text{ m}^{-1} \quad (4)$$

Using this and the previous documented data in Eq. 3 yields an average temperature rise of 0.0055 °C. Application of Eq. 1 indicates a pressure wave of magnitude 0.24 Pa through the sample.

This relatively strong thermal acoustic wave could be directly detected by a piezoelectric detector, where the signal in volts would be:

$$S = TRP \quad (5)$$

where T is the fraction of energy transmitted through the sample/detector interface, R is the responsivity of the detector measured in V/Pa, and P is the pressure generated in the sample. The fraction of energy transmitted depends on the impedances Z_s and Z_t of the sample and transducer, respectively:

$$T = \frac{4Z_s Z_t}{(Z_s + Z_t)^2} \quad (6)$$

Impedances can be calculated from

$$Z = \sqrt{\rho B} \quad (7)$$

The impedance of the detector (a monolithic solid) is $1 \times 10^6 \text{ g/cm}^2\text{-s}$ while that of a granulated solid is estimated to be $1 \times 10^4 \text{ g/cm}^2\text{-s}$ (about an order of magnitude lower than for a liquid). Thus, T is about 0.01 (1%) and, for a transducer with R of about $3.5 \times 10^{-3} \text{ V/Pa}$, yields a signal of $8 \text{ } \mu\text{V}$, which is only a little less than the thermal acoustic signals measured in Phase I of this project. However, the sample must be securely attached to the piezoelectric transducer and the transducer must be protected from incident radiation, both of which make the use of a piezoelectric transducer problematic for the on-line monitor.

On the other hand, these evaluations of the thermal elastic wave suggest that the pressure wave generated at the surface of the wall enclosing the sample could be large enough to be detected by an accelerometer. The acceleration, a , of the wall and the accelerometer attached to it is given by:

$$a = \frac{PA}{(m_t + \rho_w At)} \quad (8)$$

where m_t is the mass of the transducer, ρ_w is the density of the wall, and t is the thickness of the wall. Assuming that the mass of the wall is significantly greater than the mass of the transducer, the resulting acceleration for a steel wall of thickness 0.5 mm is:

$$a \approx \frac{P}{\rho_w t} = \frac{0.24 \text{ Pa}}{(7800 \text{ kg/m}^3)(0.5 \times 10^{-3})} = 0.0615 \text{ m/s}^2 \quad (9)$$

or, expressed in g's, the acceleration is 6.25×10^{-3} g. An inexpensive accelerometer has a sensitivity of 5.6×10^{-3} V/g; thus it would generate a signal of 35 μ V.

Thus, an accelerometer appears to be an attractive approach to detecting the thermal elastic wave in continuously moving fly ash. No gas volume is required to produce the signal and the transducer does not come into contact with the fly ash. We are pursuing a design along these lines.

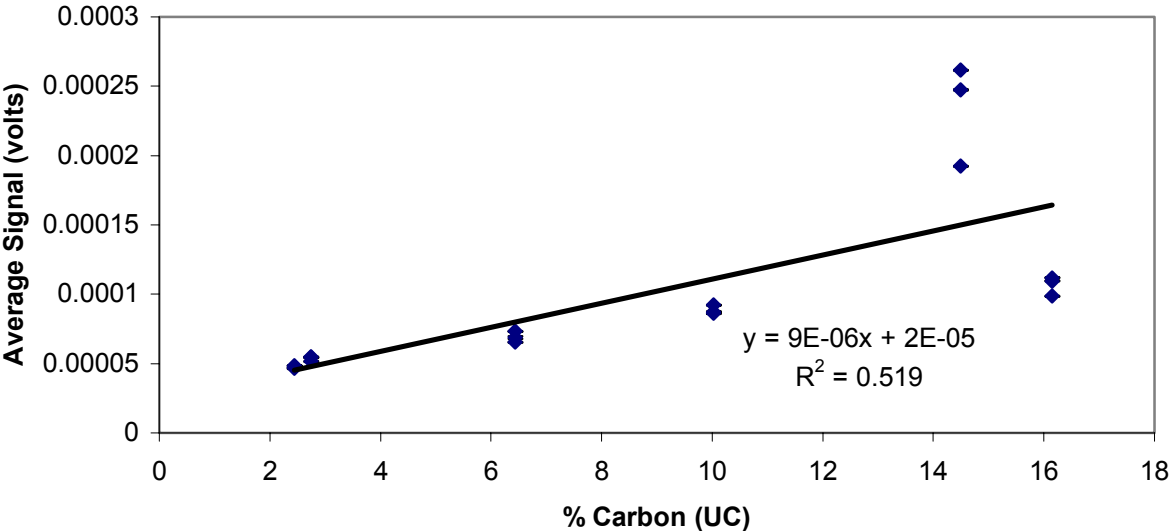
RESULTS AND DISCUSSION

The Single Microwave Frequency, Off-Line Instrument

The results for the linearity test are shown in Figure AAS1. The data set shows poor linearity due to the signals recorded for the fly ash reported to contain 14.49% carbon as determined by the Unburned Carbon methodology¹. Since photoacoustic theory suggests that under these conditions photoacoustic signal should be proportional and linear to the concentration of the absorbing material (carbon), this result was unexpected. The test was repeated and similar results were obtained. One possible explanation for the poor linearity is that the fly ash reported to contain 14.49% carbon may have other absorbing materials (such as potentially iron oxides) causing the non-linear measurements to be obtained. These fly ash samples were sent in to have Total Organic Carbon (TOC) and ash analysis tests performed on them. The results showed that there appears to be insignificant amounts of other suspected

absorbing materials in these samples.

Figure AAS1. Signal Measured for Various 3B Boiler Flyashes vs. % Carbon Using the Unburned Carbon (UC) Methodology (Test XVI: Linearity) 2/7/02



The Microwave Spectrometer

The electric field versus magnetic field setup is shown in Figure RJW-2. The source is still set at nominally 1 watt. If there were no loss in the cavity and measurement structure, then the electric field would double in the region of the sample. This would give the same results as a traveling wave of 4 watts magnitude. When the sliding short is positioned such that the electric field is at a minimum in the region of the sample, the magnetic field would be at a maximum. The VSWR pattern for nominally 0.5 dB return loss is shown below in Figure RJW-3. A sample cup is shown pictorially to scale on the center of the x-axis. Notice that the field is not zero everywhere within the cup. It will be at a minimum value for the setup but not zero. If the center of the chart represents an electric field minimum, then notice that the field magnitude is approximately 0.1 compared to just less than 2 for the maximum value. For a return loss of 0.5 dB, the field maximum would be 1.944 normalized. The ratio between the maximum electric

field to minimum electric field would be on the order of 20 giving a power ratio of 400. The expected photo-acoustic signal would be expected to be some 26 dB lower. Notice that the maximums are much flatter and cover nearly uniformly the region of the sample cup.

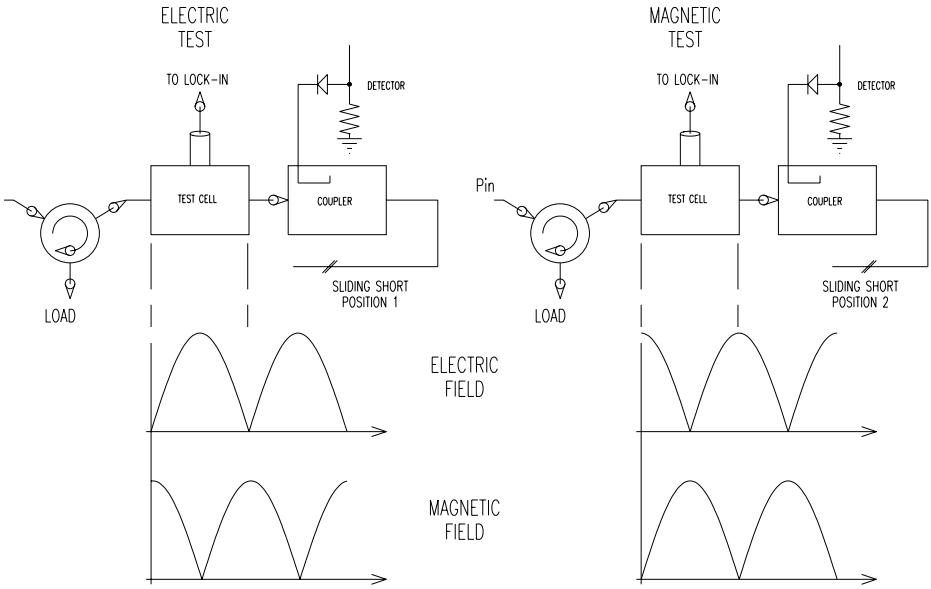


Figure RJW-2:

Electric or Magnetic Field Measurements depending on the position of the sliding short.

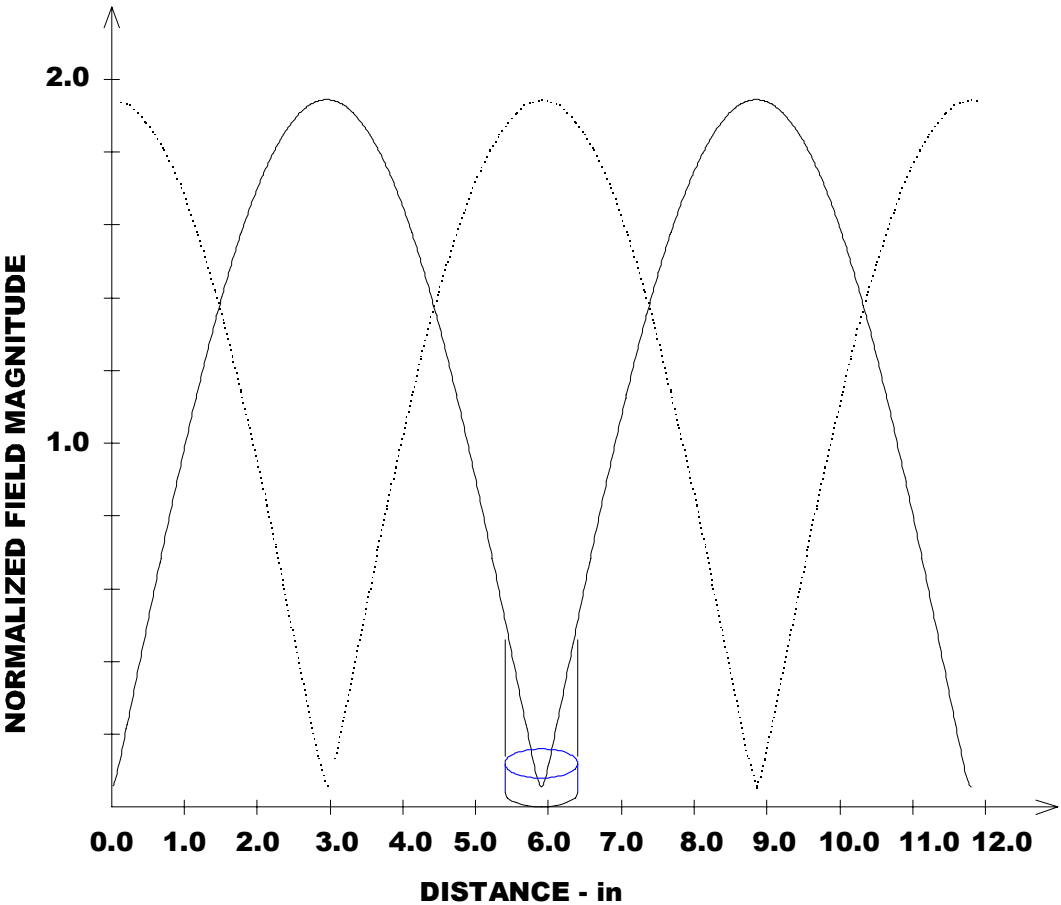


Figure RJW-3:

Electric and Magnetic field patterns at 1 GHz in relation to sample cup size.

Several sample data tests were taken with fly ash and with cobalt iron ferrite. Several frequencies in the 925 MHz to 1000 GHz range were used. The range was limited to that range for the magnetic field versus electric field tests by the bandwidth of the circulator. Figure RJW-4 shows the primarily electric and magnetic field responses for the fly ash. These curves use a post-processing signal running average of ten samples per average.

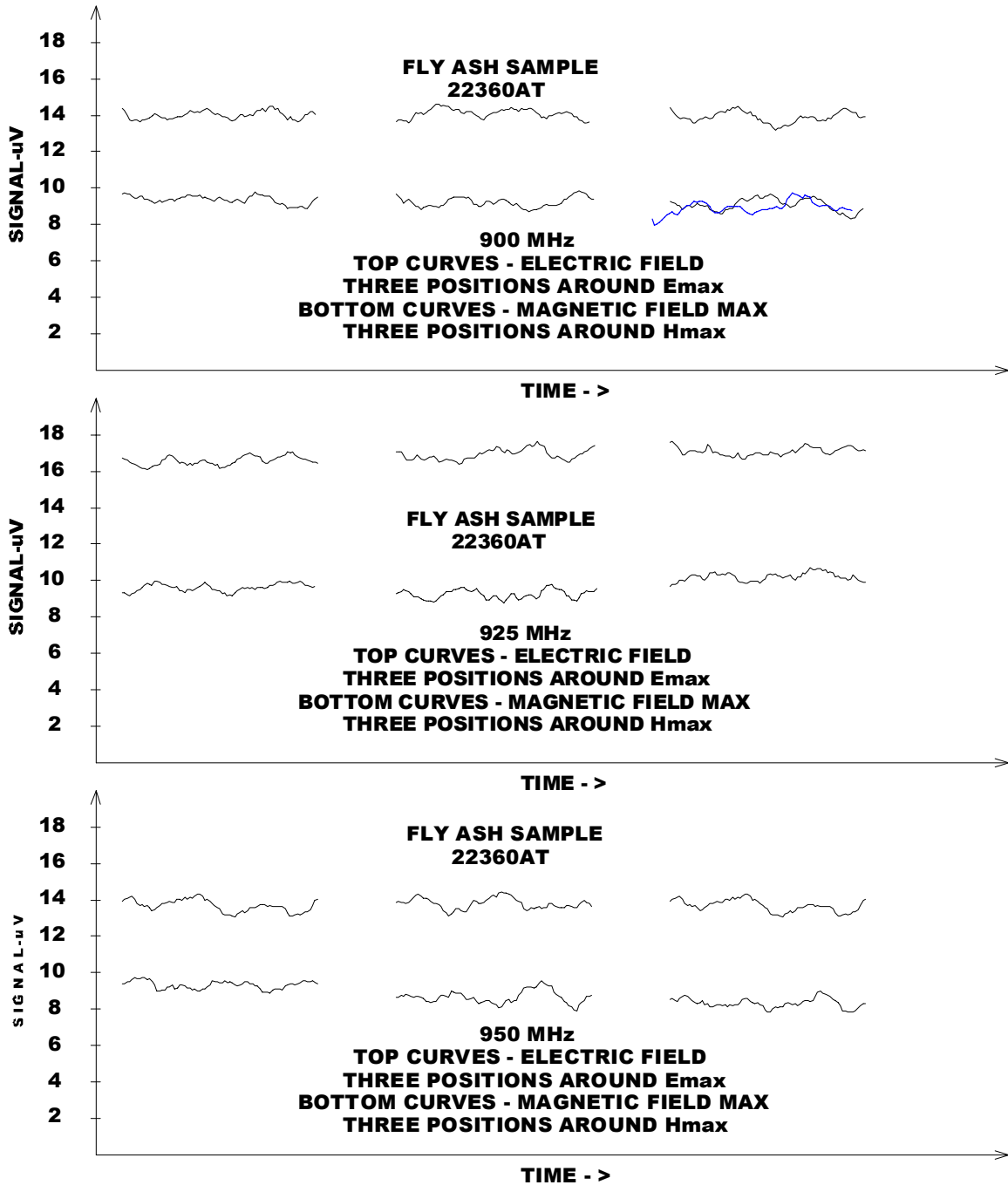


Figure RJW-4:

Photo-acoustic measurements for primarily Electric or Magnetic Field
in the region of the sample holder.

Three positions around the peak values for each data type.

The curves in Figure RJW-4 demonstrate that the photo-acoustic effect is significantly different for a peak electric field magnitude as compared to a minimum electric field. While that is not surprising, what the curves show is that there is not a large magnetic field loss. A larger magnetic field loss would be evident when the peak electric field is minimum. The magnetic field in this structure is at a maximum when the electric field is at a minimum.

Several runs were taken with a cobalt iron ferrite. That data is shown in Figure RJW-5. There is not as large of a photo-acoustic effect from the peak electric field as there is from the fly ash. That is not surprising since the cobalt iron powder is expected to have good microwave characteristics. The magnetic field maximum did not show a significantly increased value for the photo-acoustic effect. Further consideration of that will be given. The magnetic resonant frequency for the ferrite needs to be determined and then these experiments repeated in the region of the magnetic resonance for the material. It is likely that 900 MHz is well removed from the magnetic resonance frequency.

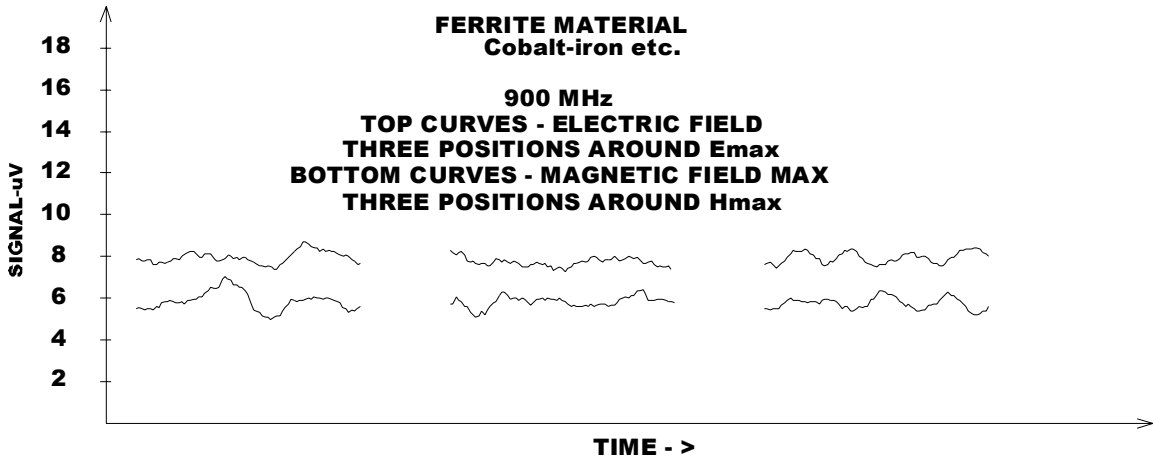


Figure RJW-5: Data for cobalt iron ferrite.

Some consideration was given to post processing the signals from the lock-in amplifier. While the lock-in amplifier bandwidth can be set to a lower frequency, it would often be desirable to have an agile post processing capability. This would allow use of post processing

signal processing to remove installation specific noise. Figure RJW-6 shows what a running average does to the signal from the lock-in amplifier. A ten point running average was used for the data that was displayed in the graphs shown above. The different running averages allow one to see what might be in the data. While it is not a certainty that there is a periodic noise in the measurement, when the data is given a five point running average, the high frequency noise is removed showing the possibility of a low frequency signal in the measurement. Further averaging the signal removes that low frequency pseudo-periodic signal. A post processing running average is similar to passing the analog signal through an analog low pass filter. The cut-off frequency of the equivalent filter goes down as the number of points in the running average goes up. If a particular environment had a large acoustical signal at some particular frequency, post processing signal processing using band reject digital filters could be applied to minimize the effect of the background noise.

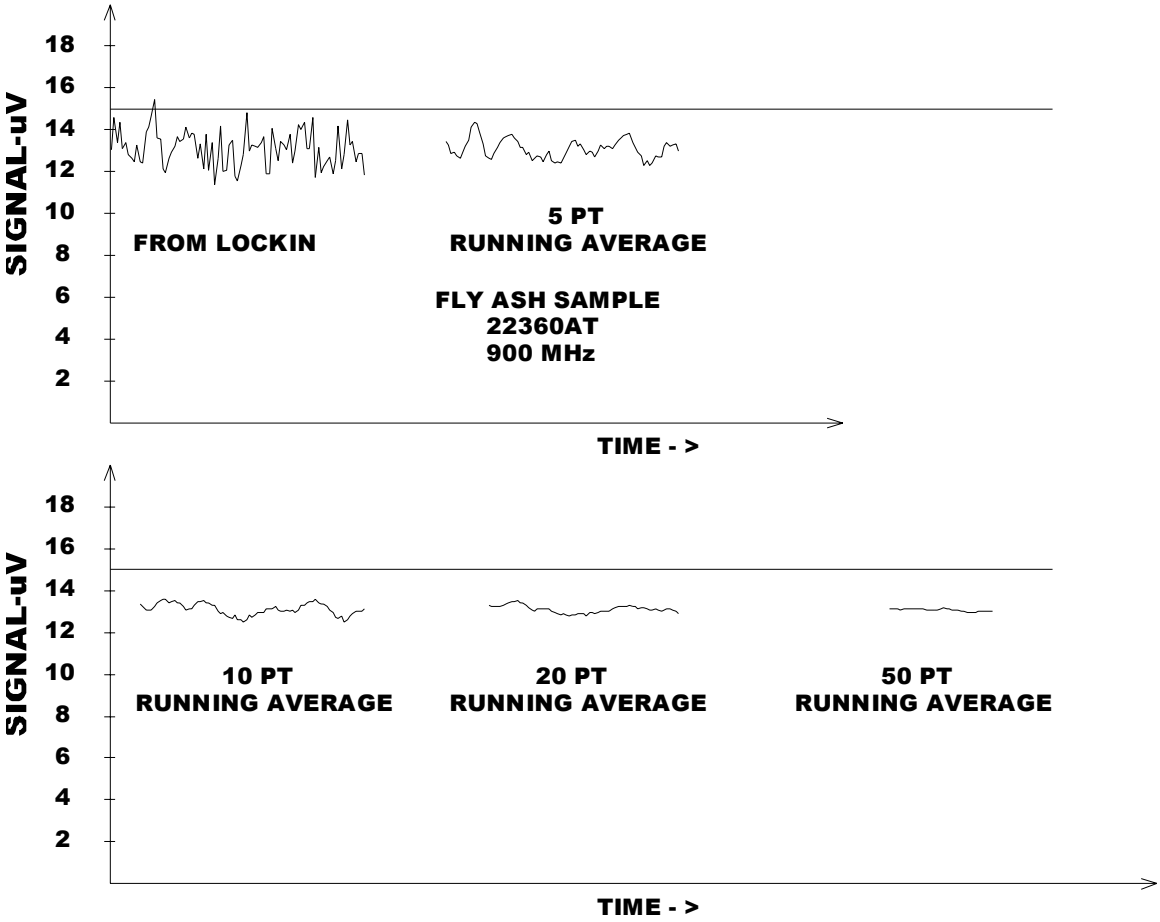


Figure RJW-6:

Running average post signal processing of the lock-in amplifier signals.

The On-line Monitor

The first iterations of these design drawings are complete and round one of revisions have been made. A design change will be implemented to overcome the possibility on non-TEM modes being experienced in the cell. The stripling configuration will be altered slightly, but the same technology will be employed.

CONCLUSION

It appears that the sample properties are not the source of any major variations in signal. As a final effort to determine the reason for signal variation, a control loop designed for the spectrometer is being used with the single frequency instrument to determine if unstable microwave power could be the source of any unexplained variations in the measurements taken date. Upon completion of this testing, Task 1 will draw to a close.

For the next quarter, efforts will focus on tests to determine the magnetic resonant frequency of the ferrite will be made. If the magnetic resonant frequency is within the frequency range capabilities of the spectrometer, tests will be performed at that frequency to determine if there is a magnetic photo-acoustic effect. Those data would be useful to determine whether there is any magnetic material contained in the fly ash. Specific frequencies for expected contaminants from various types of burners would be sought. Magnetic resonant frequencies from ferrite types of materials would be expected in the 100's of MHz to low GHz range. Dielectric loss in that frequency range would be expected to be without resonant behavior since most dielectric resonances would be at much higher millimeter wavelength frequencies. Some chemical structures such as the hydroxyl and amide bonds would be expected to give significant loss at microwave frequencies but the resonant (high loss) frequencies would be above the microwave frequency range.

During the next quarter we anticipate performing some preliminary measurements on some coal samples. We will also complete, finalize and begin construction on the on-line monitor.

REFERENCES

¹ Brown, R.C. Private Communication, Iowa State University, Ames, 2000.

APPENDIX A

SYSTEM TEST SETUP

GENERAL INFORMATION

VERSION: 1.0

Principle Investigator: Brown (Suby), Weber
Test Group: NETL (DOE)
Test Name: TestXVI
Expected duration of test: 3 hours

Date: 1/31/02
Phone: (515) 382-9006
E-mail: asuby@iastate.edu
Program: Lock-in2.bas, PAS.xls
Data: Public Private

Description of test: Linearity.

- Select 6 fly ashes of different carbon content from the 3B boiler.
- ***Perform the following procedures 3 times for each flyash:
- Weigh and record the weight of the empty sample holder.
- Fill the sample holder with sample and compress the sample as described in the produres entitled "Filling the Sample Holder" (SampleSOP.doc) and "Compressing a Fly ash Sample" (CompSampSOP.doc).
- Measure and record PA volume (depth) and weigh and record the holder and sample.
- Measure PA signal, and dump sample back into original sample bottle.
- Clean sample holder throughly with compressed air.

Objective of test: To assemble a PA signal vs. carbon curve and determine linearity

Variables under consideration: Carbon Content

Variables to be held constant: PA Volume, Sample Temp and Humidity (assumed), Ambient Temp and Humidity (assumed), Modulation Frequency

SPECIAL REQUIREMENTS

SYSTEM SETUP

DATA COLLECTED BY: NL

SAMPLE INFORMATION:

Sample Designation: See Notes:

Sample Preparation:

- "As Received" (no preparation)
- Compressed
- Ground
- Dried

Notes:

Recommend the following fly ash: 21960AT, 22332AT, 22339AT, 22342AT, 22360AT, and 22368AT

Deliverables:

- 1) Plot PA signal vs carbon content

SYSTEM INFORMATION:

Modulation Frequency: 20
Raw Data File Naming Convention:
1) Refer to the Document Entitled "Raw Data File Naming Convention for the Lock-in Data Acquisition System" (DOSDataCon.doc)

Notes:

- 1) Refer to the system Standard Operating Procedures (SystemSOP.doc)